Quinones Electrochemistry in Room-Temperature Ionic Liquids

Viktoriya A. Nikitina,*,† Renat R. Nazmutdinov,‡ and Galina A. Tsirlina†

Department of Electrochemistry, Moscow State University, Leninskie Gory 1-str. 3, 119991 Moscow, Russian Federation, and Kazan State Technological University, K. Marx Str., 68, 420015 Kazan, Republic Tatarstan, Russian Federation

Received: October 6, 2010; Revised Manuscript Received: December 1, 2010

The two-step electrochemical reduction of tetrachloro-1,2-benzoquinone (chloranil), 2-methyl-1,2-benzoquinone (toluquinone), and 9,10-anthraquinone in two room-temperature ionic liquids is addressed by means of voltammetry on a platinum electrode. For the subsequent quinone/radical anion ($Q/Q^{\bullet-}$) and radical anion/dianion ($Q^{\bullet-}/Q^{2-}$) redox reactions, the experimental data on formal potentials in 1-butyl-3-methylimidazolium tetrafluoroborate ([C_4mim][BF_4]) and 1-butyl-3-methylimidazolium hexafluorophosphate ([C_4mim][PF_6]) and literature data for the same reactants in various aprotic molecular solvents are considered in the framework of a common potential sequence (Fc^+/Fc scale) and compared with solvation energies computed at various levels. For the $Q/Q^{\bullet-}$ couple, the agreement appeared to be satisfactory when solvation is described at the polarized continuum model (PCM) level. In contrast, for the $Q^{\bullet-}/Q^{2-}$ couple, the account for specific solvation at the molecular level is crucial.

Introduction

Research in the field of electrochemical applications of room-temperature ionic liquids (RTILs) does not include a basic understanding of electron transfer (ET) kinetics in these media. At this stage, attempts to apply the models worked out for ET[1,2] and solvation[3] in molecular solvents typically fail.[4,5] It is necessary to go step by step and either construct some specific qualitatively predictive models or understand better how to choose key parameters for an appropriate application of known models. First, it is of major significance to evaluate in detail to what extent the electrochemical thermodynamics of RTIL solutions differs from that in traditional solutions.

Taking into account the RTIL heterogeneity induced by ion pairing and aggregation,[6−10] the solvent effect of these media in processes involving charged reactants might be rather specific. Before one starts to consider ET kinetics, it is crucial to ascertain the solute (reactant and product) environment. Its difference in RTILs and molecular liquids and the corresponding differences in solvation free energies are of fundamental importance because solvation is responsible for redox potential values.

On the experimental side, attempts to analyze the electrochemistry of various transition-metal-based redox couples in RTILs inevitably encounter the problem of metal ion speciation.[11−15] This is why some organic redox systems escaping complexation seem to be advantageous for a quantitative treatment of redox potentials.

We consider below just the reactants of this type, substituted quinones. The electrochemistry of these compounds in molecular solvents is quite well understood.[16,17] The reduction of quinones in aprotic solvents as well as in the presence of some proton donors occurs in two well-resolved steps first forming the radical anion, $Q^{\bullet-}$, and, at more negative potentials, the dianion, Q^{2-} (reactions 1 and 2):

$$Q^0 + e^- \leftrightarrow Q^{\bullet-} \quad (1)$$

$$Q^{\bullet-} + e^- \leftrightarrow Q^{2-} \quad (2)$$

In traditional organic solvents, the difference in the standard potentials for redox systems 1 and 2 approaches a few hundred millivolts. Both redox potentials basically depend on solvent polarity and the nature of the supporting electrolyte, reflecting both electrostatic and specific solvation energies (including ion-pairing and proton-related equilibria). In particular, hydrogen bonding and protonation induce a positive shift of redox potentials, which is much more pronounced for couple 2.[18]

Rigorous data on the formal potentials of a wide variety of substituted quinones in a large number of organic solvents are available for comparison with RTIL-based systems as well as numerous computational results on standard redox potentials of substituted quinone compounds in molecular solvents.[19−22] No similar results concerning RTIL media have been reported to date.

We present below a comparative experimental and computational study of tetrachloro-1,2-benzoquinone (chloranil) (a), 2-methyl-1,2-benzoquinone (toluquinone) (b), and 9,10-anthraquinone (c) reduction; see Figure 1 for molecular structures. 1-Butyl-3-methylimidazolium tetrafluoroborate ([C_4mim][BF_4], (d,e)) and 1-butyl-3-methylimidazolium hexafluorophosphate ([C_4mim][PF_6], (d, f)) RTILs are applied as well-characterized RTIL media.

Experimental and Computational Details

Chemicals. 1-Butyl-3-methylimidazolium tetrafluoroborate ([C_4mim][BF_4], synthesis grade) was purchased from Aldrich and stored under vacuum prior to electrochemical experiments. 1-Butyl-3-methylimidazolium hexafluorophosphate ([C_4mim][PF_6], high-purity grade, Merck) was used as received. Ferrocene ($Fe(C_5H_5)_2$, Fc, Fluka, 99%) as a reference system and tetrachloro-1,2-benzoquinone (chloranil, Acros, 99%) were used as received. 9,10-Anthraquinone was prepared according to ref 23,

* Corresponding author. Fax: +7(495)932-8846. Tel: +7(495)939-1321. E-mail: nikitina@elch.chem.msu.ru.
† Moscow State University.
‡ Kazan State Technological University.

10.1021/jp1095807
Published on Web 12/14/2010

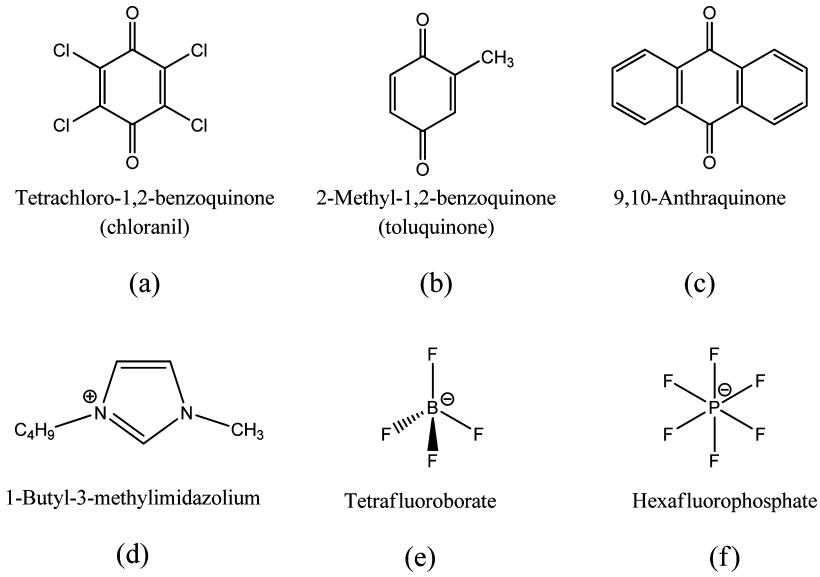

Figure 1. Reactants (a−c) and ionic components of RTILs (d−f) under study.

recrystallized twice from ethanol, and thoroughly dried. 2-Methyl-1,2-benzoquinone (toluquinone, Acros, 97%) was sublimed under vacuum twice.

Instrumentation. All of the hygroscopic substances were handled in an argon-filled glovebox with a continuous gas purification apparatus (MBRAUN Glovebox Systems). The concentrations of H_2O and O_2 in the gas never exceeded 0.1 ppm. The preparation of solutions of quinones in RTILs and the filling of the cell and its hermetization (using APIEZON grease) took place in the same glovebox. Prior to solution preparation, RTIL samples were kept under vacuum (10^{-4} mbar) for 24 h. The weight of the reactants was determined outside of the glovebox within an accuracy of 0.1 mg, resulting in a solution concentration accuracy of ca. 0.1 mM.

All electrochemical measurements were performed in a self-made three-electrode cell with a single compartment (300 μL working volume). Platinum wires (0.06 and 0.5−1 cm^2) were used as working and counter electrodes, and the third platinum wire (0.07 cm^2) was used as a quasi-reference electrode (Pt QRE). The real surface areas of the electrodes were determined from hydrogen desorption charge in aqueous 0.5 M H_2SO_4 using the same unseparated cell. No distortions of CVs were found in this case (i.e., the simplified cell geometry did not affect the quality of the data). In a number of experiments, ferrocene (Fc) was added to the solutions as an internal standard to provide a more definite potential reference. All potentials are reported below with respect to the Fc^+/Fc half-wave potential, $E_{1/2} = (E_{pa} + E_{pc})/2$ where E_{pc} and E_{pa} are the cathodic and anodic peak potentials, respectively, unless otherwise stated. For Fc voltammetry, see Figure S1a−d. A small drift in the QRE potential during the course of electrochemical measurements never exceeded 5 mV, indicating the acceptable stability of Pt QRE in RTILs under study. The accuracy of all potential values reported in this article is ca. 10 mV.

Cyclic voltammetry experiments were conducted using a computerized Autolab PGSTAT302N potentio/galvanostat (Eco-Chemie, Netherlands). To compensate for the ohmic drop, the solution resistance was estimated from Fc cyclic voltammetry under the assumption that the Fc behavior in both RTILs under study is reversible.[24−27] From the deviation of the experimental $E_{pa} - E_{pc}$ from 59 mV, the resistance of the Fc solution was estimated to be 425 and 2700 Ω for $[C_4mim][BF_4]$ and $[C_4mim][PF_6]$, respectively. All voltammograms of quinones reported below are corrected for this resistance.

Computational Details. Quantum chemistry calculations were performed at the density functional theory (DFT) level with the B3LYP hybrid functional as implemented in the Gaussian 03 program suite.[28] The geometry optimization of substituted quinones and RTIL ion pairs was performed by employing the standard split-valence triple-ζ 6-311G basis set augmented by polarization (d, p) orbitals (6-311G(d,p)). Test calculations demonstrated that the total energies of the systems under study change slightly with the enlargement of the basis set. The differences in energies computed for quinone-RTIL clusters employing 6-311++G(d,p) and 6-311G(d,p) basis sets were less than 5×10^{-4} kJ mol^{-1} for neutral and radical anion species and less than 5 kJ mol^{-1} for the quinone dianion. Thus, employing a basis set without diffuse functions does not influence potential calculations significantly. (The resulting error is estimated to be less than 50 mV.)

The zero-point energies and thermal corrections together with entropies have been used to convert the internal energies to Gibbs energies at 298.15 K.

The bulk solvation effects were addressed by including one or two RTIL ion pairs in the first coordination shell of the reacting species (a supramolecular approach) as well as on the basis of the self-consistent reaction field method (SCRF). The polarized continuum model (PCM) (e.g., refs 29−31) was employed to estimate the electrostatic contribution to the solvation energy. Estimations of solvation energies on the basis of the COSMO[32] and SCIPCM[33] models showed no significant differences in energy values as compared to calculations in the framework of the PCM model. The geometry of quinone-RTIL clusters was fully optimized without symmetry constrains, and frequency analysis has been applied to confirm that the optimized structures correspond to local minima, not transition structures. Computed bond lengths and intramolecular angles of $[C_4mim]^+[BF_4]^-$ and $[C_4mim]^+[PF_6]^-$ ion pairs are in excellent agreement with the results of previous calculations[34−36] and X-ray diffraction data.[37]

Results and Discussion

Experimental Data. ***Cyclic Voltammetry of Neat RTILs and Potential Scale Calibration.*** This section is assumed to explain the reliability of experimental potential values because

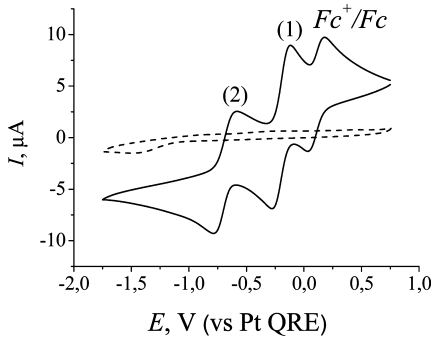

Figure 2. Cyclic voltammogram of 15 mM chloranil in $[C_4mim][BF_4]$ with the addition of 5 mM Fc (−) and the background response (---). Scan rate: 100 mV s^{-1}. Potentials are given vs Pt QRE, and the working electrode true surface area is 0.06 cm^2.

the problem of potential measurements in any melt, including RTILs, remains disputable. This problem is closely related to the impurity content, especially when a quasi-reference is used.

The potential window is a sensitive tool for controlling the impurities, especially water.[38] For $[C_4mim][BF_4]$ and $[C_4mim][PF_6]$, these windows appeared to be 4.1 and 3.5 V wide, respectively (current density cutoff values of 7×10^{-5} and 5×10^{-5} A cm^{-2}; see Figure S1e in the Supporting Information). The background current inside the windows approached 3×10^{-5} A cm^{-2} in $[C_4mim][BF_4]$ and 2.5×10^{-5} A cm^{-2} in $[C_4mim][PF_6]$. These values are in good agreement with the data on these RTILs published in refs 24, 38, and 39 under similar vacuum-dried conditions (water content <0.05%): windows of ca. 4.1 and 3.8 V with a higher (1 mA cm^{-2}) cutoff; background currents of ca. 5×10^{-5} A cm^{-2} in $[C_4mim][BF_4]$ and 2.5×10^{-5} A cm^{-2} in $[C_4mim][PF_6]$. The quality of the employed RTILs can guarantee the reliable quantitative voltammetry of electroactive species when the reactant concentration is 10 mM or higher, assuming single-electron transfer.

The ferrocene/ferrocenium redox couple has been employed for potential-scale calibration in RTILs under study. For example, Figure 2 shows a cyclic voltammogram (CV) of chloranil in $[C_4mim][BF_4]$ with 5 mM of ferrocene added to the working solution. The electrochemical features of reference and quinone couples are well resolved, so it is possible to obtain the values of redox potentials of the selected quinones directly versus the Fc^+/Fc redox couple. Formal potentials of the Fc^+/Fc couple in $[C_4mim][BF_4]$ and $[C_4mim][PF_6]$ RTILs are equal to 0.19 and 0.15 V vs Pt QRE, respectively.

Cyclic Voltammetry of Quinones. All quinones studied show two reduction peaks in RTILs as well as in nonaqueous aprotic media, corresponding to two single-electron reductions (1 and 2). The ratio of the cathodic peak current to the anodic peak current, I_{pc}/I_{pa}, for the first redox process is close to unity for

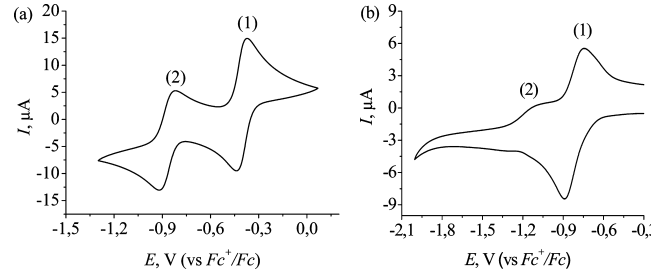

Figure 4. Cyclic voltammograms of 10 mM chloranil (a) and 24.5 mM toluquinone (b) in $[C_4mim][PF_6]$. The scan rate is 100 mV s^{-1}, and the potential is measured vs Pt QRE and recalculated on the Fc^+/Fc scale.

all of the quinones throughout the scan rate, v, range from 25 to 400 mV s^{-1}. The same ratio for the second redox process was found to be below unity.

The behavior of chloranil in RTILs $[C_4mim][BF_4]$ and $[C_4mim][PF_6]$ is illustrated in Figures 3a and 4a. For the first pair of peaks (assigned to the reversible reduction of chloranil to its radical anion), the peak-to-peak separation at slow scan rates was close to 60 mV. The second pair of peaks demonstrated quasi-reversible behavior, with the peak-to-peak separation varying from 95 to 115 mV in $[C_4mim][BF_4]$ and from 90 to 112 mV in $[C_4mim][PF_6]$ with increasing v. With I_{pc} and I_{pa} determined using the baseline corresponding to the current at the formal potential, the I_{pc}/I_{pa} ratio was 0.7−0.8.

The electrochemical behavior of toluquinone appeared to be more complicated (Figures 3b and 4b). In contrast to chloranil CVs, the current decreased during cycling, probably indicating a strong adsorption of the reactant on the surface of the platinum electrode in $[C_4mim][BF_4]$. The first pair of peaks behaved quasi-reversibly, with the peak-to-peak separation varying from 95 to 111 mV. A very pronounced discrepancy in both I_{pc} and I_{pa} for two subsequent redox processes could point to a significantly lower diffusion coefficient for the quinone dianion or to some mechanistic complications arising from possible specific adsorption. Peak-to-peak separation for the redox reaction involving the dianion and radical anion reached ca. 200 mV. The situation is quite similar for the $[C_4mim][PF_6]$ RTIL. We failed to obtain quantitative information concerning the redox potential of process 2 in the $[C_4mim][PF_6]$ RTIL because of less reproducible behavior in subsequent cycles, probably resulting from the accumulation of adsorbed products.

Figure 3c shows a cyclic voltammogram of anthraquinone in the $[C_4mim][BF_4]$ RTIL. The peak-to-peak separation for redox process 1 varies from 75 to 100 mV with a scan rate increase in the above-mentioned interval, thus indicating a quasi-reversible reaction. The peak-to-peak separation reaches 140 mV for redox process 2. The discrepancy in the values of I_{pc}

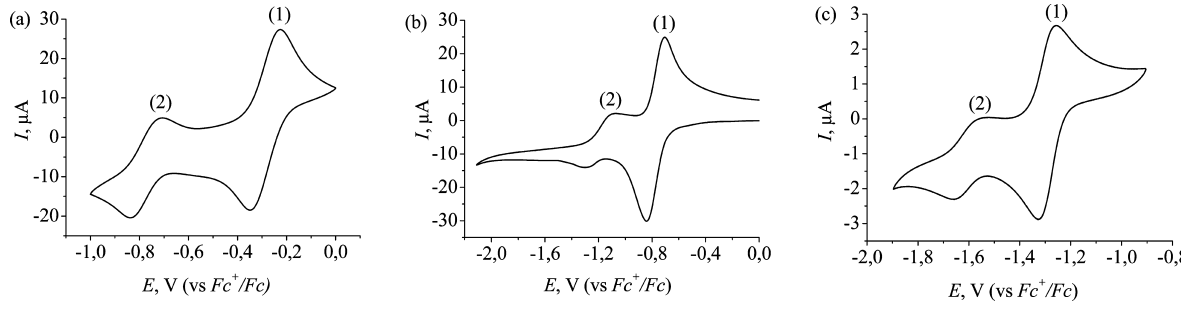

Figure 3. Cyclic voltammograms of 25 mM chloranil (a), 20 mM toluquinone (b), and 8 mM anthraquinone in $[C_4mim][BF_4]$ (c). The scan rate is 100 mV s^{-1}, and the potential is measured vs Pt QRE and recalculated on the Fc^+/Fc scale.

TABLE 1: Formal Potentials of Redox Processes (1) (E_1, V) and (2) (E_2, V) vs Fc^+/Fc for a Series of Quinone Compounds in RTILs [C_4mim][BF_4] and [C_4mim][PF_6] and Diffusion Coefficients (D, $cm^2\ s^{-1}$) for Neutral Quinones and Radical Anions, Which Are Assumed To Be Equal

reactant	solvent	E_1	E_2	$D(Q) \times 10^8$
chloranil	[C_4mim][BF_4]	−0.28	−0.78	2.6
	[C_4mim][PF_6]	−0.30 (2)	−0.79 (1)	1.0
toluquinone	[C_4mim][BF_4]	−0.77	−0.95	3.6
	[C_4mim][PF_6]	−0.82	∼−1.0	
anthraquinone	[C_4mim][BF_4]	−1.13	−1.48	2.0

and I_{pa} for processes 1 and 2 is also to be noted. Because of the low solubility of anthraquinone in the [C_4mim][PF_6] RTIL, we were unable to obtain quantitative voltammetry for this RTIL.

The lower currents for couple 2 as compared to those for couple 1 were observed for all quinones, with the effect being the most pronounced for toluquinone. Among several possible explanations considered, the assumption concerning a complexation reaction between a quinone and its dianion looks the most realistic:[17,18]

$$Q + Q^{2-} \leftrightarrow [QQ]^{2-} \quad (3)$$

We should note that whereas this suggested complexation reaction accounts very well for the difference in peak heights, it turns out to have no pronounced effect on the formal potentials of the two waves and therefore does not introduce any uncertainty in further comparisons with calculated potentials.

The $I_p(\nu^{1/2})$ dependencies remained linear for chloranil in both RTILs in the overall υ interval, indicating that the reaction is diffusion-controlled (Figure S2a,b). For anthraquinone and toluquinone, the linearity was not maintained at high scan rates (>200 mV s^{-1}) because of the quasireversible behavior of these quinone-based redox systems (Figure S2c,d). In this case, the diffusion coefficients were determined from the linear part of the $I_p(\nu^{1/2})$ plots corresponding to low scan rates. Diffusion coefficients D obtained from cyclic voltammetry (calculated from peak currents of process 1 using the Randles−Sevcik equation[40]) are summarized in Table 1, as are the formal potentials versus the Fc^+/Fc couple.

Only minor differences in formal redox potentials can be observed in two RTILs under investigation for the same chloranil- and toluquinone-based redox couples (20 and 50 mV, respectively). Given that these RTILs contain the same cation and weakly coordinating anions, this closeness may indicate that the reacting quinone species are mainly solvated by RTIL cation components.

Solvodynamic Radii Estimates. The diffusion coefficients, D, of the reactants were employed to estimate the solvodynamic radii of the diffusing species, r_s, using the Stokes−Einstein equation

$$r_s = \frac{k_B T}{4\pi\eta D} \quad (4)$$

where k_B is the Boltzmann constant, T is the absolute temperature, and η is the viscosity of the medium. A comparison of the r_s values with the molecular radii of isolated species may provide indirect information concerning the solvation of reactants. If the solvodynamic radius value differs significantly from the size of isolated molecules, then it is reasonable to assume the strong solvation of the reactive species and even to estimate roughly the number of solvent molecules in the first solvation shell. We considered the reactants to be ellipsoids of rotation forming a cavity for the species. The effective radius of a spherical reactant was then calculated from the volume of the ellipsoid. Viscosity data for RTILs [C_4mim][BF_4] and [C_4mim][PF_6] were taken from refs 41 and 42: 110 and 275 mPa s, respectively.

TABLE 2: Effective Radii Estimated on the Basis of Ionic (r_{ion}, Å), Atomic (r_{at}, Å), and van der Waals (r_W, Å) Radii of Terminal Atoms and Solvodynamic Radii of Quinones (r_s, Å) in RTILs [C_4mim][BF_4] and [C_4mim][PF_6]

reactant	RTIL	r_{ion}	r_{at}	r_W	r_s
chloranil	[C_4mim][PF_6]	3.5	4.3	4.5	7.5
	[C_4mim][BF_4]				7.8
toluquinone	[C_4mim][BF_4]	3.3	3.9	4.1	5.5
anthraquinone	[C_4mim][BF_4]	4.1	4.7	5.0	9.9

Table 2 summarizes the effective quinone radii estimated using ionic, atomic, and van der Waals radii for terminal atoms (to take into account their volume) and also solvodynamic radii r_s calculated on the basis of eq 4. The latter significantly exceeds corresponding values of molecular radii for all isolated quinone molecules (2−5 Å).

Similar values of the solvodynamic radii of chloranil in both RTILs indicate again that mainly cations are responsible for the solvation of the reacting species. The differences in solvodynamic and calculated radii may correspond to one or two RTIL cations involved in the closest solvation shell, depending on the cation orientation. The charged forms of quinones are likely to exhibit more pronounced solvation by RTIL cations, but in this case, we avoid the determination of diffusion coefficients from the cyclic voltammetry data because process 2 is complicated by dimerization and demonstrates quasireversible behavior even at slow scan rates.

Formal Potentials: Sequences and Correlations. Formal potentials of redox processes involving the neutral quinone, radical anion, and dianion species both in the RTIL and the molecular solvent media are primarily determined by the change in the Gibbs free energy of corresponding redox reactions in solution. The solvating capability of the medium is thus responsible for the difference in formal potentials of the same reactants in different solvents.

A traditional approximation results from the assumption that Fc^+ and Fc are very weakly solvated in all solvents under discussion, including RTILs. This point can also be discussed in terms of the liquid junction potential or the free energy of transfer of the species from one solvent to another. No reliable approaches are known for treating the liquid junction problem in RTIL systems. This uncertainty can be escaped when we consider not the potential value on a fixed scale but the potential separation between two successive electron-transfer reactions of a given compound in a given solvent.

The standard electrode potential of redox process 1 is determined by the difference in gas-phase (G_{gas}) and solvation (G_{solv}) energies of the radical anion and neutral quinone:

$$-FE_1 = (G_{gas}(Q^{\bullet -}) - G_{gas}(Q)) + (G_{solv}(Q^{\bullet -}) - G_{solv}(Q)) = \Delta G_{gas}(Q/Q^{\bullet -}) + \Delta G_{solv}(Q/Q^{\bullet -}) \quad (5)$$

For the formal potential of redox process 2, one can similarly write

$$-FE_2 = (G_{gas}(Q^{2-}) - G_{gas}(Q^{\bullet-})) + (G_{solv}(Q^{2-}) - G_{solv}(Q^{\bullet-})) = \Delta G_{gas}(Q^{\bullet-}/Q^{2-}) + \Delta G_{solv}(Q^{\bullet-}/Q^{2-}) \quad (6)$$

An estimate of the electrostatic contribution to the solvation energy may be obtained using solvation models based on self-consistent reaction field (SCRF) methods. The polarized continuum model (PCM) is one of the most commonly applied SCRF models, with the solvent being represented as a dielectric continuum with permittivity ε. In the PCM, the solvation energy is partitioned into four components: the electrostatic interaction, a cavity term, and dispersion and repulsion energies (with the last three terms representing nonelectrostatic interactions between the solute and solvent).

Table 3 summarizes PCM solvation energies, G_{solv}, of reduced and oxidized forms of quinones under study, which are estimated on the basis of PCM in six organic solvents [acetonitrile (AN), benzonitrile (BN), dimethylsulfoxide (DMSO), *N*,*N*-dimethylacetamide (DMA), propylene carbonate (PC), and *N*,*N*-dimethylformamide (DMF)] as well as in RTIL [C_4mim][BF_4]. Because the solvation energy values estimated using the SCRF formalism primarily depend on the dielectric permittivity value of the solvent, we concentrate mainly on the construction of potential sequences for reactants in the [C_4mim][BF_4] RTIL because of very similar dielectric permittivity values in the RTILs under study[43] and the less complicated behavior of quinones in [C_4mim][BF_4] compared to that in the [C_4mim][PF_6] RTIL.

On the basis of computed solvation energies and gas-phase energy differences of quinones, potential values for systems 1 and 2 were calculated. To obtain calculated electrode potentials versus the potential of the Fc^+/Fc redox couple, the value of 4.44 V was taken as the absolute potential of the standard hydrogen electrode (SHE), and the potential of Fc^+/Fc was assumed to be 0.4 V vs SHE.[44]

Table 4 summarizes the calculated potential values and provides a comparison with experimental data taken from ref 45.

Figures 5−7 show formal potential sequences evaluated experimentally (a, c) and computed on the basis of the PCM formalism (b, d) for the quinones under study.

It must be noted that the adopted procedure for the calculation of redox potentials of quinone-based systems in molecular solvents involves the assumption that the supporting electrolyte dissolved in an organic solvent plays no role in solvation because its concentration is much lower than that of the dipolar solvent. However, because of the extremely low conductivity of many molecular solvents, rather high concentrations of electrolyte are typically used and both the radical anion and dianion can undergo ion-pairing stabilization. Therefore, experimental potentials turn out to be more positive than calculated with the ignorance of this effect for

TABLE 3: PCM Solvation Energies (G_{solv}, kJ mol^{-1}) for Neutral Quinones ($z = 0$), Radical Anions ($z = -1$), and Dianions ($z = -2$) in [C_4mim][BF_4] (IL) and Several Organic Solvents [Acetonitrile (AN), Benzonitrile (BN), Dimethyl Sulfoxide (DMSO), Dimethylacetamide (DMA), Propylene Carbonate (PC), and Dimethylformamide (DMF)]

reactant	z	G_{solv} (IL)	G_{solv} (AN)	G_{solv} (BN)	G_{solv} (DMSO)	G_{solv} (DMA)	G_{solv} (PC)	G_{solv} (DMF)
chloranil	0	−25	−27	−27	−20	−20	−29	−20
	−1	−174	−191	−179	−183	−182	−184	−182
	−2	−734	−781	−754	−785	−765	−773	−764
toluquinone	0	−18	−19	−19	−20	−20	−20	−20
	−1	−201	−214	−211	−216	−214	−217	−214
	−2	−748	−795	−785	−800	−796	−806	−795
anthraquinone	0	−18	−21	−21	−21	−21	−21	−21
	−1	−184	−196	−194	−199	−197	−200	−197
	−2	−659	−703	−693	−708	−704	−713	−703

TABLE 4: Calculated (E_1^{calc} and E_2^{calc}, V) and Experimental (E_1^{exp} and E_2^{exp}, V) Electrode Potentials for Redox Systems 1 and 2 vs Fc^+/Fc and Differences in Formal Potentials for Processes 1 and 2 (ΔE_{1-2}^{exp} and ΔE_{1-2}^{calc}, V) in Several Solvents ([C_4mim][BF_4] (IL), Acetonitrile (AN), Benzonitrile (BN), Dimethyl Sulfoxide (DMSO), Dimethylacetamide (DMA), Propylene Carbonate (PC), and Dimethylformamide (DMF))[a]

reactant	solvent	E_1^{calc}	E_1^{exp}	E_2^{calc}	E_2^{exp}	ΔE_{1-2}^{exp}	ΔE_{1-2}^{calc}
chloranil	[C_4mim][BF_4]	−0.39	−0.28	−1.22	−0.78	0.50	0.83
	AN	−0.23	−0.16	−0.91	−0.95	0.79	0.68
	PC	−0.33	−0.17	−0.92	−0.88	0.71	0.59
	DMF	−0.26	−0.13	−0.99	−1.04	0.91	0.73
	DMSO	−0.25	−0.12	−0.79	−0.95	0.82	0.54
	BN	−0.36	−0.17	−1.06	−0.93	0.77	0.70
	DMA	−0.26	−0.12	−0.98	−1.05	0.94	0.73
toluquinone	[C_4mim][BF_4]	−1.17	−0.77	−3.00	−0.95	0.18	1.84
	AN	−1.05	−0.76	−2.65	−1.50	0.74	1.60
	PC	−1.02	−0.77	−2.57	−1.27	0.49	1.55
	DMF	−1.05	−0.74	−2.65	−1.65	0.92	1.60
	DMSO	−1.03	−0.70	−2.61	−1.59	0.90	1.58
	BN	−1.07	−0.76	−2.73	−1.37	0.61	1.65
	DMA	−1.04	−0.75	−2.64			1.60
anthraquinone	[C_4mim][BF_4]	−1.57	−1.14	−2.95	−1.48	0.34	1.38
	AN	−1.46	−1.11	−2.64	−1.65	0.55	1.18
	PC	−1.43	−1.12	−2.56	−1.45	0.33	1.13
	DMF	−1.46	−1.08	−2.63	−1.82	0.74	1.18
	DMSO	−1.44	−1.03	−2.60	−1.75	0.72	1.15
	BN	−1.48	−1.12	−2.70	−1.56	0.44	1.22
	DMA	−1.45	−1.05	−2.63	−1.77	0.71	1.17

[a] Experimental formal potential values in molecular organic solvents are taken from ref 45.

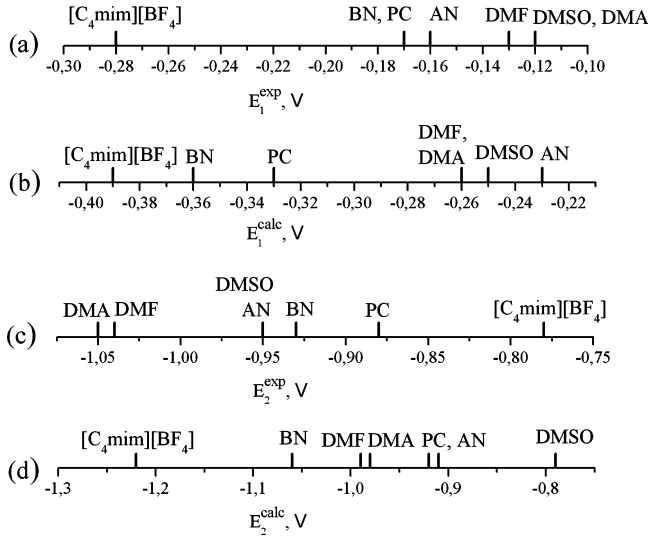

Figure 5. Sequences of formal potentials for chloranil-based redox systems 1 and 2, determined experimentally (E_1^{exp} and E_2^{exp}, panels a and c, respectively) and computed on the basis of the PCM solvation model (E_1^{calc} and E_2^{calc}, panels b and d, respectively) in [C_4mim][BF_4] and molecular solvents acetonitrile (AN), benzonitrile (BN), dimethyl sulfoxide (DMSO), dimethylacetamide (DMA), propylene carbonate (PC), and dimethylformamide (DMF).

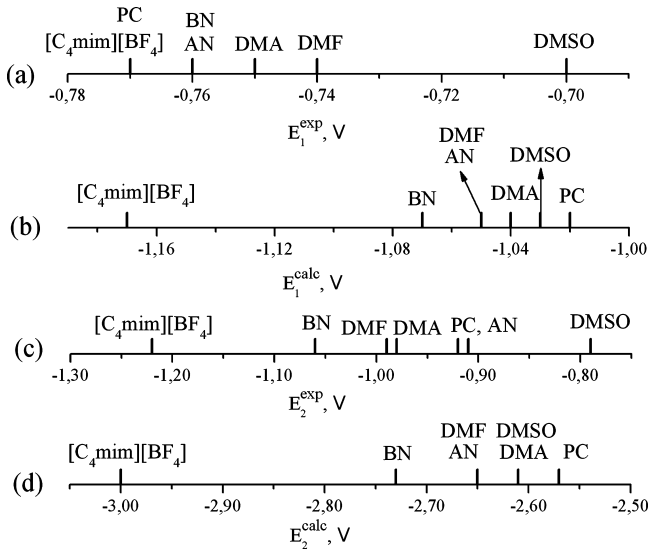

Figure 6. Sequences of formal potentials for toluquinone-based redox systems 1 and 2, determined experimentally (E_1^{exp} and E_2^{exp}, panels a and c, respectively) and computed on the basis of the PCM solvation model (E_1^{calc} and E_2^{calc}, panels b and d, respectively) in [C_4mim][BF_4] and molecular solvents acetonitrile (AN), benzonitrile (BN), dimethyl sulfoxide (DMSO), dimethylacetamide (DMA), propylene carbonate (PC), and dimethylformamide (DMF).

all of the reactants under study. However, this complication is not expected to influence the sequences of calculated and experimental potentials.

Basically all calculated potential series correlate with an experimental series for redox processes involving uncharged quinone and radical anion species, with the most significant deviations being demonstrated for chloranil in acetonitrile and for toluquinone and anthraquinone in propylene carbonate. This fact may point to the existence of the most pronounced specific solvation of the systems under study in two respective solvents.

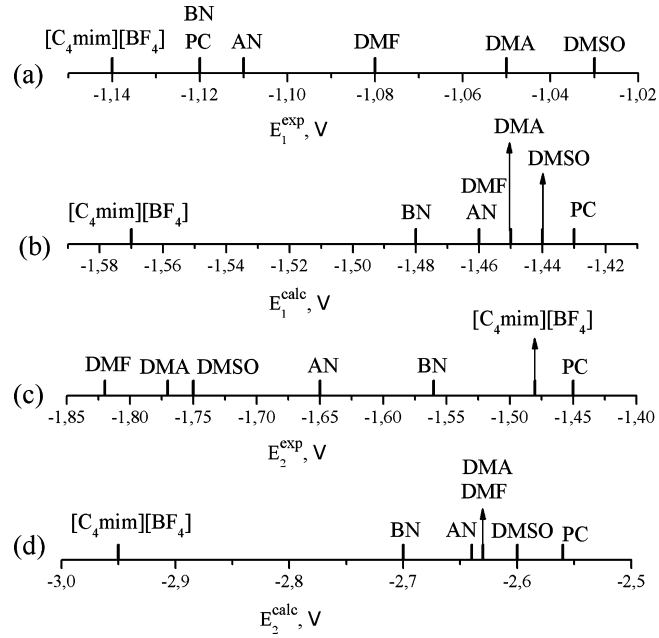

Figure 7. Sequences of formal potentials for anthraquinone-based redox systems 1 and 2, determined experimentally (E_1^{exp} and E_2^{exp}, panels a and c, respectively) and computed on the basis of the PCM solvation model (E_1^{calc} and E_2^{calc}, panels b and d, respectively) in [C_4mim][BF_4] and molecular solvents acetonitrile (AN), benzonitrile (BN), dimethyl sulfoxide (DMSO), dimethylacetamide (DMA), propylene carbonate (PC), and dimethylformamide (DMF).

Interestingly, the calculated potential values for all of the quinones in RTIL media are the most negative in the corresponding series. This supports the assumption of the weak solvation of neutral and radical anion species, with the solvation energy thus being determined mostly by the electrostatic component evaluated in the framework of the PCM. Given the extremely low dielectric permittivity of [C_4mim][BF_4] (~12), the minimal solvation energy of reactants and hence the most negative potential value is more or less predictable.

The calculated potential sequences do not correlate with experimental formal potentials for redox process 2. Experimental values for RTIL media are the most positive in the potential sequence, with the potential separation for the two reduction processes being minimal, whereas the SCRF formalism predicts the most negative potential in the series and the largest potential separation.

Thus, simple electrostatic solvation models are hardly applicable to treat complex solute−solvent interactions of highly charged quinone species and RTIL components. It should be noted that experimental and calculated potential series for redox process 2 show only a weak correlation for molecular solvents. This may point to complex specific nonelectrostatic interactions that are present in the molecular solvent/quinone system, with the effect however being more pronounced for RTILs.

Cluster Description of Quinone Solvation. An alternative description of quinone specific solvation in RTIL-based systems can be implemented on the basis of the quantum chemical description of model clusters containing RTIL molecules and quinone species. Chloranil was chosen as a model quinone compound because of the less complicated electrochemical behavior in RTILs compared to that of other quinones under study. Molecular clusters consisting of one or two ionic liquid units and neutral, radical anion, or dianion chloranil species have

TABLE 5: Gibbs Free Energies for Quinone-RTIL and RTIL Clusters in the Gas Phase (G_{gas}, h) and Calculated Electrostatic (G_{PCM}, kJ mol^{-1}) and Specific (ΔG_{chem}, kJ mol^{-1}) Solvation Energy Components and Total Solvation Energies (G_{solv}^{tot}, kJ mol^{-1})

cluster	G_{gas}	G_{PCM}	ΔG_{chem}	G_{solv}^{tot}
$[Q-IL]^0$	−3067.892	−26	6	−20
$[Q-IL]^{-1}$	−3068.016	−174	−36	−210
$[Q-IL]^{-2}$	−3068.001	−665	−204	−869
$[Q-2IL]^0$	−3915.805	−26	−24	−50
$[Q-2IL]^{-1}$	−3915.921	−174	−44	−218
$[Q-2IL]^{-2}$	−3915.902	−665	−202	−867
1RTIL	−847.887			
2RTIL	−1695.788			

been fully optimized at the DFT/B3LYP 6-311G(d,p) level to obtain model solvation shells for chloranil:

$$Q^0 + n[C_4mim][BF_4] \rightarrow [Q-nIL]^0 \quad (7)$$

$$Q^{\bullet -} + n[C_4mim][BF_4] \rightarrow [Q-nIL]^{\bullet -} \quad (8)$$

$$Q^{2-} + n[C_4mim][BF_4] \rightarrow [Q-nIL]^{2-} \quad (9)$$

$n = 1, 2$.

Tables S4−S6 in the Supporting Information list Cartesian coordinates for quinone-RTIL and RTIL clusters, comprising one and two RTIL units.

Resulting optimized cluster structures for the neutral molecule and radical anion show no significant solvent rearrangement in the vicinity of the reactant molecule, indicating a weak specific contribution to the total solvation energy. The tendency is different, however, for the dianion species. Strong hydrogen bonding is predicted between negatively charged oxygen atoms of the chloranil dianion and acidic protons of the 1-butyl-3-methylimidazolium cation. It is expected that strong specific interactions shift the potential of the second redox process toward less negative potential values.

The Gibbs free energy values were computed independently for chloranil derivatives Q, $Q^{\bullet -}$, and Q^{2-} and RTIL ion pairs. For processes 7−9, this quantity was estimated as follows

$$\Delta G_{chem} = G([Q-nIL])^{0/\bullet -/2-} - G(nIL) - G(Q^{0/\bullet -/2-}) \quad (10)$$

where G is the Gibbs free energy of the corresponding species.

It should be noted that the entropy terms that we calculated using our cluster model include three main contributions resulting from the vibrational, translational, and rotational modes. These estimations are not exact because a real system most likely has a number of shallow energy minima that make an additional orientational contribution to the entropy. This effect can be properly addressed using molecular dynamics simulations. For our systems, this small error can hardly be crucial because at room temperature the entropy term is noticeably smaller than the enthalpy.

The full solvation energy of a quinone can be calculated as the sum of an electrostatic component, estimated in terms of the PCM formalism for a quinone, G_{PCM}, and specific component, ΔG_{chem}, calculated on the basis of eq 10:

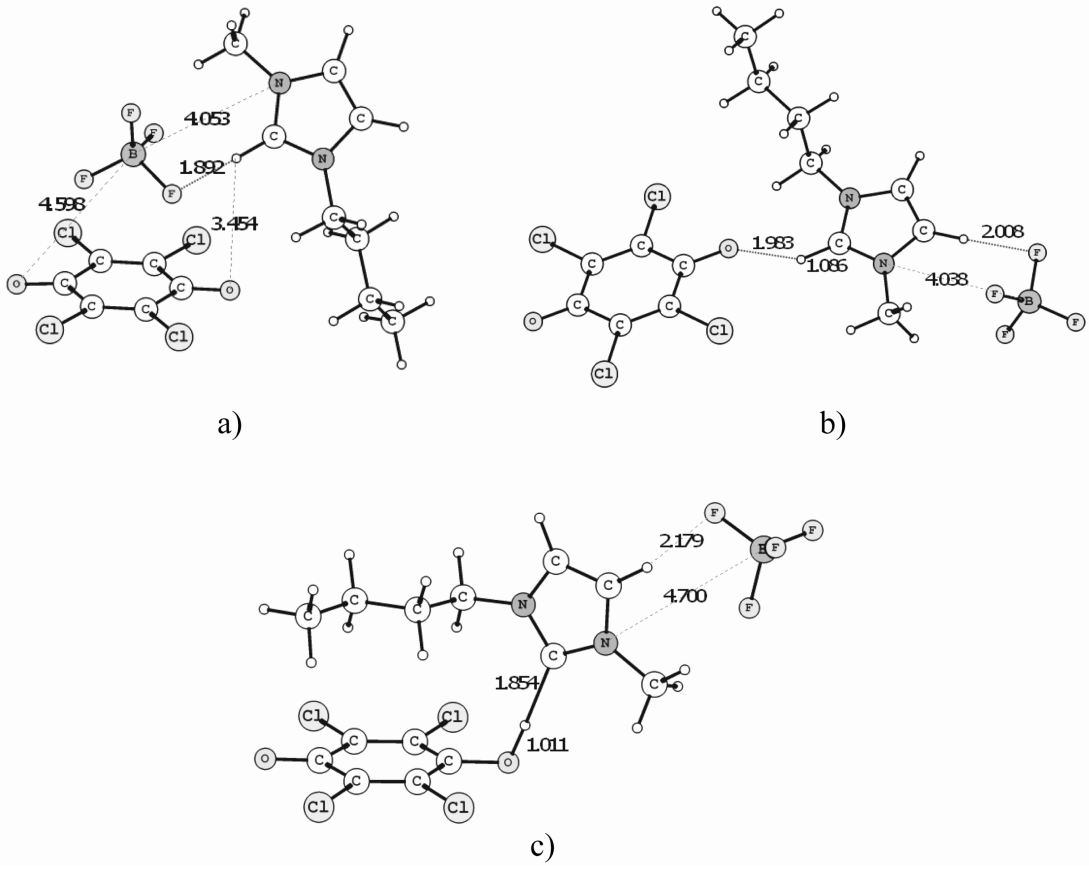

Figure 8. Optimized cluster structures $[Q-IL]^0$ (a), $[Q-IL]^{\bullet -}$ (b), and $[Q-IL]^{2-}$ (c) and some selected distances between atoms (Å).

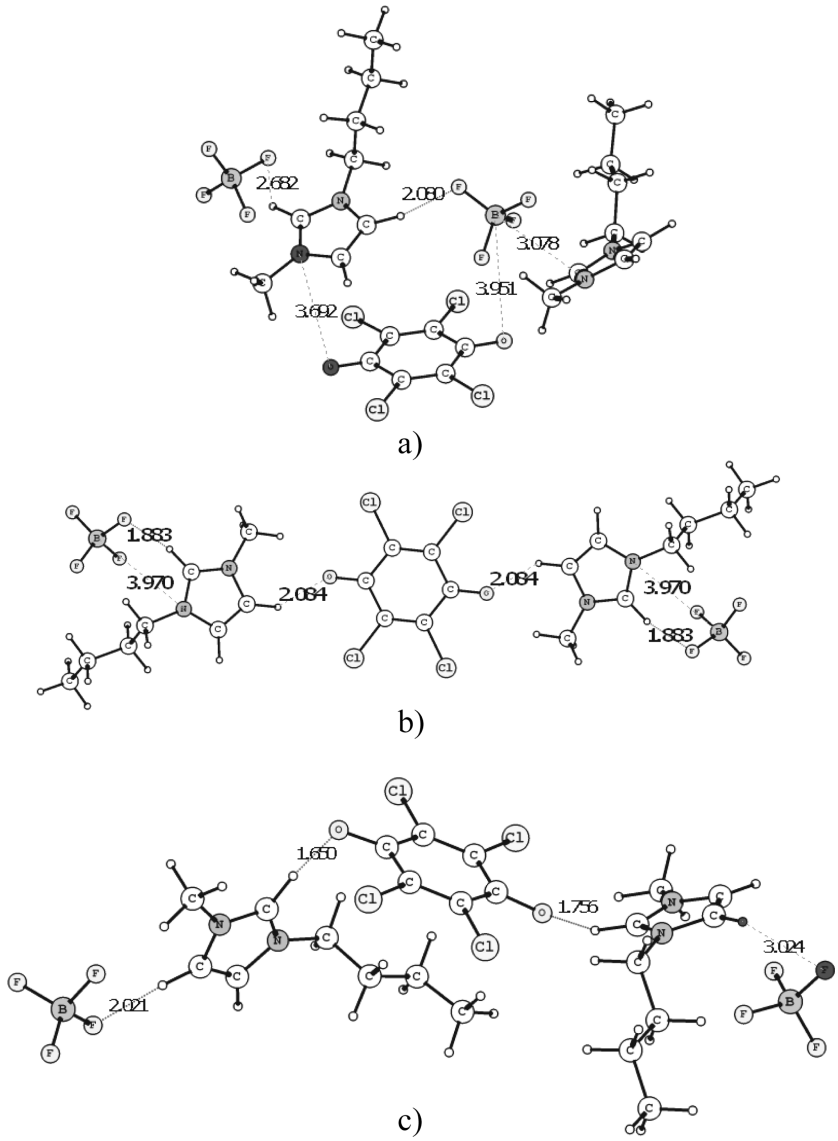

Figure 9. Optimized cluster structures $[Q-2IL]^0$ (a), $[Q-2IL]^{\cdot-}$(b), and $[Q-2IL]^{2-}$ (c) and some selected distances between atoms (Å).

$$G_{solv}^{tot}(Q) = G_{PCM} + \Delta G_{chem} \quad (11)$$

Table 5 summarizes the Gibbs free energies computed for quinone redox forms in the gas phase and in solution and the calculated specific and electrostatic contributions to the total solvation energy.

The results of calculations allow us to predict the values of specific solvation energies for neutral chloranil, the radical anion, and the dianion: 6, −36, and −204 kJ mol^{-1} for quinone clusters containing one IL molecule and −24, −44, and −202 kJ mol^{-1} for clusters comprising two RTIL units, respectively. The electrode potential calculation on the basis of full solvation energies leads to the following estimates:

- The redox potential for the $Q/Q^{\cdot-}$ system reaches 0.1 V (single RTIL clusters) and −0.1 V (two RTIL clusters) versus Fc^+/Fc (experimental value −0.28 V).

- The redox potential for the $Q^{\cdot-}/Q^{2-}$ couple reaches −0.2 V (single RTIL clusters) and −0.3 V (two RTIL clusters) versus Fc^+/Fc (experimental value −0.78 V).

For neutral chloranil and the radical anion, the difference in specific solvation energies was found to be small, which explains the good correlation between potentials calculated above on the basis of the PCM model and those determined experimentally. For the radical anion and dianion, the difference in specific solvation energies amounts to 160 kJ mol^{-1}, thus explaining the shift in the redox potential for chloranil in the RTIL medium in the positive direction in the experimental series compared to calculated values. The computed formal potential values differ greatly from those obtained experimentally, with the redox potential values for systems 1 and 2 being more positive than the experimental values. An overestimation of the specific solvation effect upon the shift in the formal potential is not surprising because our approach does not address the interaction of the molecular cluster with other ions in the solvation shell, which may reduce the solvent−solute interactions. For clusters containing two RTIL units, this overestimation is even more pronounced because of a larger number of solute−solvent contacts. The difference between the system 1 and 2 redox potential values is 200 and 100 mV for one and two RTIL molecule clusters, being smaller than the experimental value (ca. 500 mV). Thus, whereas the applied approach qualitatively predicts a positive shift in the formal potential, more realistic specific solvation energies can be obtained only on the basis of

complete solvation shell modeling, which can be accomplished on the basis of MD simulations (e.g., ref 46). However, a quantitative treatment of the systems under study goes beyond the scope of this article.

Conclusions

For the first time, we reported redox potentials for a series of quinone compounds (chloranil, toluquinone, and anthraquinone in RTILs $[C_4mim][BF_4]$ and $[C_4mim][PF_6]$), data on the reversibility, and diffusion coefficients obtained from cyclic voltammetry measurements. Redox processes involving radical anion and neutral quinone species are reversible for chloranil and quasireversible for toluquinone and anthraquinone. Redox processes involving the radical anion and dianion are quasireversible for all of the quinones. Solvodynamic radii were estimated from diffusion coefficients obtained from the Stokes−Einstein equation and were compared with geometrical molecular dimensions, computed using the DFT formalism. The difference in the values obtained was interpreted in terms of solvation shell formation.

It was demonstrated that potential sequences calculated in the framework of the PCM for the $Q/Q^{\bullet-}$ redox process correlate with experimental formal potential sequences for all quinones under study. This indicates that specific solvation-energy values differ only slightly for the neutral molecule and radical anion of a quinone compound. Such a correlation is not observed for process involving the radical anion and dianion. The specific solvation energy of redox-active quinone forms in the RTIL medium was computed in terms of the microscopic treatment of the system under study, which involved the modeling of RTIL-quinone clusters. Our calculations predict specific solvation energy values for neutral chloranil, the radical anion, and the dianion to be equal to 6, −36, and −204 kJ mol^{-1} for quinone clusters containing one RTIL molecule and −24, −44, and −202 kJ mol^{-1} for clusters comprising two RTIL units, respectively. The large specific interaction energy between the dianion and the RTIL cation can by attributed to the hydrogen bond formation between oxygen atoms of chloranil and acidic protons of the imidazolium rings. The calculation of electrode potentials using computed energy values experimentally predicts the observed shift of quinone-based redox system potentials toward less negative values.

It is pointed out, therefore, that the potential shift toward positive values upon the transition from molecular solvents to RTILs can be explained on the basis of specific solvation-energy estimates for reactants in RTIL media. At the current stage of describing complex solvent−solute interactions, the prediction of the behavior of solvents in the series can serve as evidence of the applicability of the microscopic quinone solvation model for ionic liquid media.

Acknowledgment. This work was supported by the RFBR (project no. 08-03-00915-a). We are grateful to Prof. R. Buchner from Regensburg University and Prof. W. R. Fawcett from the University of California, Davis, for stimulating discussions.

Supporting Information Available: Cyclic voltammetry of ferrocene and quinone derivatives. Geometrical parameters of quinones and quinone-RTIL clusters. This material is available free of charge via the Internet at http://pubs.acs.org.

References and Notes

(1) Nazmutdinov, R. R.; Tsirlina, G. A.; Petrii, O. A.; Kharkats, Y. I.; Kuznetsov, A. M. *Electrochim. Acta* **2000**, *45*, 3521–3536.
(2) Zagrebin, P. A.; Buchner, R.; Nazmutdinov, R. R.; Tsirlina, G. A. *J. Phys. Chem. B* **2010**, *114*, 311–320.
(3) Zagrebin, P. A.; Nazmutdinov, R. R.; Spector, E. A.; Borzenko, M.; Tsirlina, G. A.; Mikhelson, K. N. *Electrochim. Acta* **2010**, *55*, 6064–6072.
(4) Lynden-Bell, R. M. *J. Phys. Chem. B* **2007**, *111*, 10800–10806.
(5) Kobrak, M. N.; Li, H. *Phys. Chem. Chem. Phys.* **2010**, *12*, 1922–1932.
(6) Tokuda, H.; Tsuzuki, S.; Susan, M. A. B. H.; Hayamizu, K.; Watanabe, M. *Phys. Chem. B* **2006**, *110*, 19593–19600.
(7) Xiao, D.; Rajian, J. R.; Cady, A.; Li, S.; Bartsch, R. A.; Quitevis, E. L. *J. Phys. Chem. B* **2007**, *111*, 4669–4677.
(8) Hunt, P. A.; Gould, I. R.; Kirchner, B. *Aust. J. Chem.* **2007**, *60*, 9–14.
(9) Katoh, R.; Hara, M.; Tsuzuki, S. *J. Phys. Chem. B* **2008**, *112*, 15426–15430.
(10) Wulf, A.; Fumino, K.; Ludwig, R. *Angew. Chem., Int. Ed.* **2010**, *49*, 449–453.
(11) Tachikawa, N.; Serizawa, N.; Katayama, Y.; Miura, T. *Electrochim. Acta* **2008**, *53*, 6530–6534.
(12) Matsumiya, M.; Suda, S.; Tsunashima, K.; Sugiya, M.; Kishioka, S.; Matsuura, H. *J. Electroanal. Chem.* **2008**, *622*, 129–135.
(13) Yamagata, M.; Tachikawa, N.; Katayama, Y.; Miura, T. *Electrochim. Acta* **2007**, *52*, 3317–3322.
(14) Yamagata, M.; Katayama, Y.; Miura, T. *J. Electrochem. Soc.* **2006**, *153*, E5−E9.
(15) Mukhopadhyay, I.; Aravinda, C. L.; Borissov, D.; Freyland, W. *Electrochim. Acta* **2005**, *50*, 1275–1281.
(16) Chambers, J. Q. *The Chemistry of the Quininoid Compounds*; Wiley: New York, 1988; Vol. 2.
(17) Lehmann, M. W.; Evans, D. H. *J. Electroanal. Chem.* **2001**, *500*, 12–20.
(18) Gupta, N.; Linschitz, H. *J. Am. Chem. Soc.* **1997**, *119*, 6384–6391.
(19) Riahi, S.; Eynollahi, S.; Ganjali, M. R. *Int. J. Electrochem. Sci.* **2009**, *4*, 1128–1137.
(20) Namazian, M.; Norouzi, P.; Ranjbar, R. *J. Mol. Struct.: THEOCHEM* **2003**, *625*, 235–241.
(21) Namazian, M.; Almodarresieh, H. A. *J. Mol. Struct.: THEOCHEM* **2004**, *686*, 97–102.
(22) Namazian, M. *J. Mol. Struct.: THEOCHEM* **2003**, *664−665*, 273–278.
(23) Senseman, C. E.; Nelson, O. A. *Ind. Eng. Chem.* **1923**, *15*, 521–524.
(24) Hultgren, V.; Mariotti, A.; Bond, A.; Wedd, A. *Anal. Chem.* **2002**, *74*, 3151–3156.
(25) Waligora, L.; Lewandowski, A.; Gritzner, G. *Electrochim. Acta* **2009**, *54*, 1414–1419.
(26) Shiddiky, M.; Torriero, A.; Zhao, C.; Burgar, I.; Kennedy, G.; Bond, A. *J. Am. Chem. Soc.* **2009**, *131*, 7976–7989.
(27) Rogers, E.; Silvester, D.; Poole, D.; Aldous, L.; Hardacre, C.; Compton, R. *J. Phys. Chem. C* **2008**, *112*, 2729–2735.
(28) Frisch, M. J.; Trucks, G. W.; Schlegel, H. B.; Scuseria, G. E.; Robb, M. A.; Cheeseman, J. R.; Montgomery, J. A. J.; Vreven, T.; Kudin, K. N.; Burant, J. C.; Millam, J. M.; Iyengar, S. S.; Tomasi, J.; Barone, V.; Mennucci, B.; Cossi, M.; Scalmani, G.; Rega, N.; Petersson, G. A.; Nakatsuji, H.; Hada, M.; Ehara, M.; Toyota, K.; Fukuda, R.; Hasegawa, J.; Ishida, M.; Nakajima, T.; Honda, Y.; Kitao, O.; Nakai, H.; Klene, M.; Li, X.; Knox, J. E.; Hratchian, H. P.; Cross, J. B.; Bakken, V.; Adamo, C.; Jaramillo, J.; Gomperts, R.; Stratmann, R. E.; Yazyev, O.; Austin, A. J.; Cammi, R.; Pomelli, C.; Ochterski, J. W.; Ayala, P. Y.; Morokuma, K.; Voth, G. A.; Salvador, P.; Dannenberg, J. J.; Zakrzewski, V. G.; Dapprich, S.; Daniels, A. D.; Strain, M. C.; Farkas, O.; Malick, D. K.; Rabuck, A. D.; Raghavachari, K.; Foresman, J. B.; Ortiz, J. V.; Cui, Q.; Baboul, A. G.; Clifford, S.; Cioslowski, J.; Stefanov, B. B.; Liu, A. L.; Piskorz, P.; Komaromi, I.; Martin, R. L.; Fox, D. J.; Keith, T.; Al-Laham, M. A.; Peng, C. Y.; Nanayakkara, A.; Challacombe, M.; Gill, P. M. W.; Johnson, B.; Chen, W.; Wong, M. W.; Gonzalez, C.; Pople, J. A. *Gaussian 03, Revision C.02*; Gaussian, Inc.: Wallingford, CT, 2004.
(29) Cances, E.; Menucci, B.; Tomasi, J. *J. Chem. Phys.* **1997**, *107*, 3032–3042.
(30) Menucci, B.; Cammi, R.; Tomasi, J. *J. Chem. Phys.* **1999**, *110*, 6858–6870.
(31) Tomasi, J.; Persico, M. *Chem. Rev.* **1994**, *94*, 2027–2094.
(32) Klamt, A.; Schüürmann, G. *J. Chem. Soc., Perkin Trans. 2* **1993**, 799–805.
(33) Foresman, J. B.; Keith, T. A.; Wiberg, K. B.; Snoonian, J.; Frisch, M. J. *J. Phys. Chem.* **1996**, *100*, 16098–16104.
(34) Hunt, P.; Gould, I.; Kirchner, B. *Aust. J. Chem.* **2007**, *60*, 9–14.
(35) Antony, J.; Mertens, D.; Breitenstein, T.; Dölle, A.; Wasserscheid, P.; Carper, W. *Pure Appl. Chem.* **2004**, *76*, 255–261.
(36) Meng, Z.; Dolle, A.; Carper, W. *J. Mol. Struct.: THEOCHEM* **2002**, *585*, 119–128.
(37) Dibrov, S. M.; Kochi, J. K. *Acta Cryst.,* **2006**, *C62*, o19−o21.

(38) O'Mahony, A. M.; Silvester, D. S.; Aldous, L.; Hardacre, C.; Compton, R. G. *J. Chem. Eng. Data* **2008**, *53*, 2884–2891.
(39) Schroder, U.; Wadhawan, J. D.; Compton, R. G.; Marken, F.; Suarez, P. A. Z.; Consorti, C. S.; Souza, R. F.; Dupont, J. *New J. Chem.* **2000**, *24*, 1009–1015.
(40) Bard, A. J.; Faulkner, L. R. *Electrochemical Methods, Fundamental and Applications*, 2nd ed.; Wiley: New York, 2001.
(41) Wang, J.; Tian, Y.; Zhao, Y.; Zhuo, K. *Green Chem.* **2003**, *5*, 618–622.
(42) Buzzeo, M. C.; Evans, R. G.; Compton, R. G. *Chem. Phys. Chem.* **2004**, *5*, 1106–1120.
(43) Stoppa, A.; Hunger, J.; Buchner, R. *J. Phys. Chem. B* **2008**, *112*, 4854–4858.
(44) Trasatti, S. *Pure Appl. Chem.* **1986**, *58*, 955–966.
(45) Sasaki, K.; Kashimura, T.; Ohura, M.; Ohsaki, Y.; Ohta, N. *J. Electrochem. Soc.* **1990**, *137*, 2437–2443.
(46) VandeVondele, J.; Sulpizi, M.; Sprik, M. *Angew. Chem.* **2006**, *118*, 1970–1972.

JP1095807